CASE 42

Gas-Arc Stud Weld Process Parameter Optimization Using Robust Design

Abstract: This paper describes a parameter design experiment utilized to optimize a gas-arc stud welding process. The desired outcome of the project was to determine the optimum process parameter levels leading to minimized variation and maximized stud weld strength across a wide array of real-world processing conditions. The L_{18} orthogonal array experiment employed a zero-point proportional dynamic SN ratio, with signal levels varying across runs. The optimized process parameters yielded a confirmed SN ratio improvement of 6.4 dB, thus reducing the system's energy transformation variability by 52%. Implementation of the optimized process parameters is expected to result in significant cost savings, due to the elimination of a secondary welding operation and a significant reduction in downstream stud strength failures.

1. Introduction

Welding Process

Stud welding is a general term for joining a metal stud to a metal base material. In *gas-arc stud welding*, the base of the stud is joined to the base material by heating both parts with an arc drawn between them and then bringing the parts together under pressure.

The typical steps in gas-arc stud welding (Figure 1) are as follows:

1. The stud is loaded into the chuck and the stud gun is positioned properly for welding by inserting the spark shield into the welding fixture bushing until the stud base contacts the workpiece.
2. The stud gun's trigger is depressed, starting the automatic welding cycle. Immediately upon triggering the weld cycle, the original atmosphere within the spark shield is purged with a controlled gas mixture. Upon purge completion the solenoid coil within the gun body becomes energized, concurrently lifting the stud off the workpiece and creating an arc.
3. The base of the stud and surface of the workpiece are melted by the arc.
4. Upon completion of the preset arc period, the welding current is shut off automatically. This deenergizes the solenoid coil, causing the gun's main spring to plunge the stud into the molten pool of the workpiece, completing the weld.
5. The controlled gas mixture continues to be applied for a specific time after deenergization to ensure the proper gas atmosphere as the weld solidifies.
6. The stud gun is removed, yielding the finished product.

Problems with the Process

Case Corporation's Racine tractor plant had been experiencing an unacceptably high level of

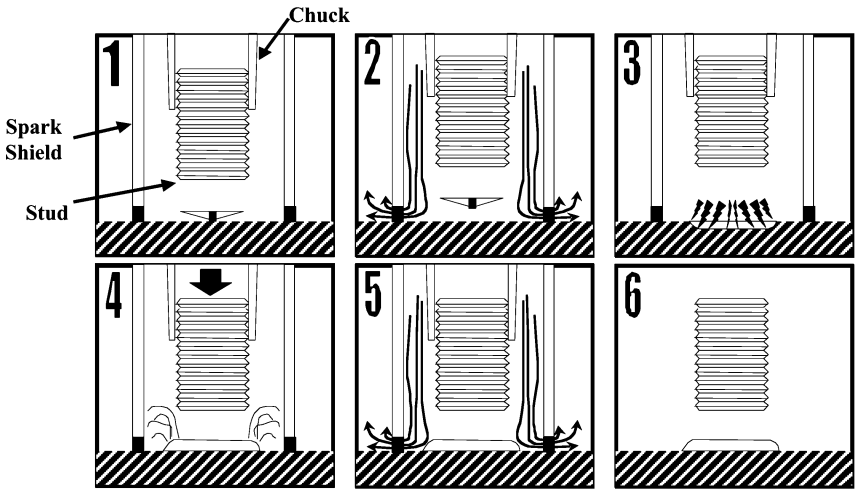

Figure 1
Gas-arc stud welding process

threaded metal studs breaking off during the tractor assembly process. Stud weld strength variation was identified as one of the primary causes of assembly breakage. To ensure adequate strength in the short term, the weld department began reinforcing each stud by adding an additional manual tack-weld step. This additional step added more cost to the process and only masked the underlying variation; therefore, an improved long-term solution was needed.

The problem-solving team decided that its first step in determining a long-term solution was to optimize the controllable parameters (control factors) of the gas-arc stud weld process using robust design methodology.

Desired Outcome

The desired outcome of the project was to determine the optimum process parameter levels, leading to minimized variation and maximized stud weld strength across a wide array of real-world processing conditions.

2. Experimental Procedure

The study was performed using studs 10 mm in diameter and 28 mm in long, of low carbon content, with a 1.5-mm thread, and 50,000 psi tensile yield strength, and HSLA ROPS steel base material.

Engineered System

The stud welding process can be broken down into an engineering system with three types of input variables and one output (response) variable (Figure 2). Each variable type is discussed in detail below.

Signal Factor

The signal factor is typically the primary energy input into the engineering system. For a gas-arc stud welding system the signal factor (M) is defined as

$$M = M_I M_T M_V$$

where M is the energy input into the system, M_I the average welding current as set on the welding power supply, M_T the welding time (arc period) as set on the welding power supply, and M_V the average peak voltage during welding as determined by the power supply's automatic feedback loop. The power supply is programmed to maintain a constant current; therefore, the voltage is adjusted automatically based on Ohm's law ($I = VR$). Thus, voltage could not be set; instead, it had to be measured for each trial.

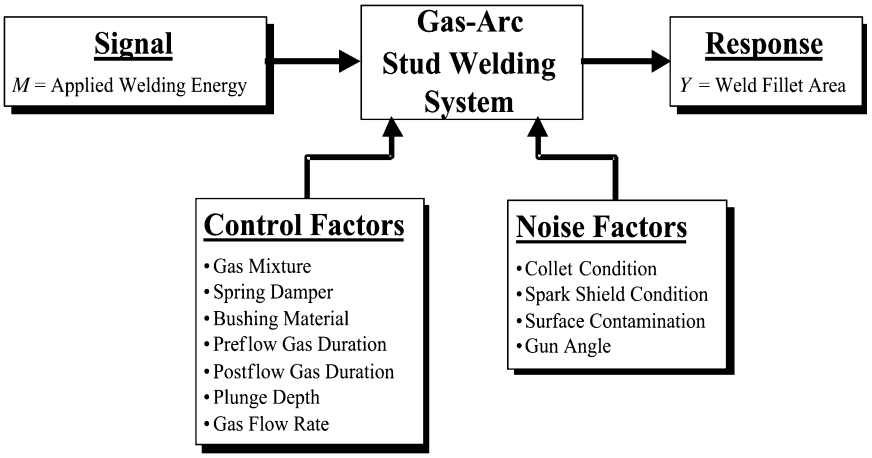

Figure 2
Engineered system

Studs were welded at nine different signal levels for each experiment run (Table 1). However, due to the inherent variation in the welding power supply, the actual values varied somewhat from the set point. Therefore, an oscilloscope was used to record actual welding current, welding time, and peak voltage for each stud welded. The actual energy input (M_i) was then calculated for each trial based on the oscilloscope readings.

Table 1
Signal factor settings

Trial	M_I: Average Current (A)	M_T: Welding Time (s)
M_1 and M_2	560	0.35
M_3 andM_4	560	0.40
M_5 and M_6	560	0.45
M_7 and M_8	700	0.35
M_9 and M_{10}	700	0.40
M_{11} and M_{12}	700	0.45
M_{13} and M_{14}	840	0.35
M_{15} and M_{16}	840	0.40
M_{17} and M_{18}	840	0.45

Response Factor

The response factor (Y) is the measurable intended output of the engineered system. The use of maximum applied torque prior to stud breakage as the response factor was considered. This approach would work well if weld strength is less than the stud material yield strength; however, it would not give an accurate indication if weld strength equaled or exceeded the stud material yield strength. In addition, it could not detect instances of excessive applied energy. Therefore, a more suitable response factor had to be found.

Based on discussions with several welding experts, it was determined that measuring the annular weld fillet area at the base of the stud would provide a reasonable estimate of the amount of energy applied to make a weld. Therefore, annular weld fillet area was chosen as the response factor (Y).

Ideal Function

In an ideal stud welding system, 100% of the welding input energy (signal) would be efficiently transformed into the weld, bonding the stud and base material. However, under real-world conditions, the efficiency of the energy transformation will vary due to the presence of noise factors. The goal of robust design is to minimize the effect of noise factors and to maximize the efficiency of the energy transformation.

The ideal function for the stud welding system is given by

$$y = \beta M$$

where y is the weld fillet area, M the welding energy, and β the slope of the best-fit line between y and M.

Noise Strategy

Noise factors cause variability in the energy transformation of the engineered system. These are factors that are difficult, impossible, or too expensive to control. Robust design strives to make the engineered system insensitive to these noise factors.

Based on brainstorming, the project team determined that the following noise factors were the most important: collet condition, spark shield condition, stud gun angle, and workpiece surface contamination. A compound noise strategy was chosen to simulate mild (N_1) and severe (N_2) noise conditions. Table 2 shows the noise factor settings for each of the compound noise levels.

Control Factors

Control factors are the parameters that can be specified by process designers. The project team's brainstorming efforts yielded the following critical factors: gas mixture, spring damper, bushing material, preflow gas duration, postflow gas duration, plunge depth, and gas flow rate.

In addition, the team felt that arc length was an important factor. However, it was excluded from the experiment because changing the arc length would increase arc resistance and thus interact significantly with the feedback control loop of the welding power supply. Therefore, based on existing engineering knowledge, the arc length was held constant at 3/32 in. for the entire experiment. Level settings for each of the control factors are shown in Table 3.

Orthogonal Array

The use of an orthogonal array allows for efficient sampling of the multidimensional design space. An L_{18} (2×3^7) orthogonal array was chosen for this experiment. The L_{18} array is shown under the inner array portion of Table 4. Each run within the inner array was repeated for each signal and noise level, as shown in the outer array portion of the table. The experiment design required a total of 324 stud welds (18 runs $\times$ 9 signal levels $\times$ 2 noise levels).

3. Results and Data Analysis

The annular weld fillet area of each stud was estimated using the methodology summarized in Figure 3. In addition, each stud was stressed to failure using a torque testing apparatus that closely simulated assembly forces. Torque testing results are presented in Table 5. Figure 4 provides a graphical comparison of annular weld fillet area versus maximum torque for all 324 welded studs. The comparison shows that the fillet area provides a good indication of the relative probability that a stud will survive the assembly torque upper specification limit (15 ft-lb for 10-mm studs).

Out of 224 studs with a fillet area larger than 34 mm^2, only one stud (run 10, M_7, N_1) failed below the assembly torque upper specification limit. This stud exhibited a large hollow fillet (>5 mm wide) on one side of the stud base and no fillet on the other side. Therefore, fillet width consistency also needs to be considered when predicting a stud's ability to survive assembly torque requirements.

Table 2
Compound noise factor settings

Noise Factor	N_1: Mild Noise	N_2: Severe Noise
Collet condition	New	Near end of useful life
Spark shield condition	New	Near end of useful life
Stud gun angle	Perpendicular	Leaning against bushing
Surface contamination	Clean part	Oil-coated part

Table 3
Control factors and levels

Control Factor		Level 1	Level 2	Level 3
A:	gas mixture	90% argon–10% CO_2	98% argon–2% O_2	—
B:	spring damper	None	Weak	Mid
C:	bushing material	Plastic	Steel	Brass
D:	preflow gas duration(s)	0.50	0.75	1.0
E:	postflow gas duration(s)	0.25	0.50	1.0
F:	plunge depth (in.)	0.040	0.070	0.100
*G**:	dummy factor (result of eliminating arc length from experiment)	—	—	—
H:	gas flow rate (ft^3/h)	10	20	30

Additionally, Figure 4 shows that the transition point between weld failure and stud material failure occurs near 20 ft-lb of applied torque.

SN Ratio

The signal-to-noise ratio (SN or η) is the best indicator of system robustness. As this ratio increases, the engineered system becomes less sensitive to noise factor influences, and the efficiency of the energy transformation increases. The goal of SN analysis is to determine the set of control factor settings that maximize the SN.

Zero-Point Proportional SN Ratio

The experiment was designed to treat the response factor (fillet area) as a zero-point proportional dynamic characteristic. The formula for a zero-point proportional SN ratio is

$$\eta = 10 \log \frac{(1/r)(S_\beta - V_e)}{V_e}$$

where $V_e = S/(k-1)$. The magnitude of the energy input (r) can be calculated as

$$r = \sum_{i=1}^{k} M_i^2$$

where M_i is the welding energy input and k is the number of input levels per run. The variation caused by the linear effect of β (S_β) can be determined as

$$S_\beta = \frac{1}{r}\left(\sum_{i=1}^{k} M_i y_i\right)^2$$

where y_i is the fillet area. To calculate the error variance (V_e), the total variation sum of squares (S_T) and error variation (S_e) need to be calculated as

$$S_T = \sum_{i=1}^{k} y_i^2$$

The error variance can now be calculated:

$$S_e = S_T - S_\beta$$

Calculation Example

The methodology used to determine the SN ratio for each experimental run is demonstrated using data from run 3. Table 6 shows the energy input (M) and fillet area (y) data for each trial of run 3. The calculations used to determine the SN ratio (η) for run 3 are shown below.

$$r = M_1^2 + M_2^2 + \cdots + M_{18}^2 = 6232^2 + 6611^2 + \cdots + 15365^2$$

$$= 2{,}158{,}878{,}662$$

Table 4
Experiment array

	Inner Array								Outer Array																	
	Control Factor Level								M_1		M_2		M_3		M_4		M_5		M_6		M_7		M_8		M_9	
Run	*A*	*B*	*C*	*D*	*E*	*F*	*G*	*H*	N_1	N_2	N_1	N_2	N_1	N_2	N_1	N_2	N_1	N_2	N_1	N_2	N_1	N_2	N_1	N_2	N_1	N_2
1	1	1	1	1	1	1	1	1																		
2	1	1	2	2	2	2	2	2																		
3	1	1	3	3	3	3	3	3																		
4	1	2	1	1	2	2	3	3																		
5	1	2	2	2	3	3	1	1																		
6	1	2	3	3	1	1	2	2																		
7	1	3	1	2	1	3	2	3																		
8	1	3	2	3	2	1	3	1																		
9	1	3	3	1	3	2	1	2																		
10	2	1	1	3	3	2	2	1																		
11	2	1	2	1	1	3	3	2																		
12	2	1	3	2	2	1	1	3																		
13	2	2	1	2	3	1	3	2																		
14	2	2	2	3	1	2	1	3																		
15	2	2	3	1	2	3	2	1																		
16	2	3	1	3	2	3	1	2																		
17	2	3	2	1	3	1	2	3																		
18	2	3	3	2	1	2	3	1																		

$$S_\beta = \frac{1}{r}\,(M_1 y_1 + M_2 y_2 + \cdots + M_{18} y_{18})^2$$

$$= \frac{1}{2{,}158{,}878{,}662}\,[(6232)(16.48) + (6611)(27.93) + \cdots + (15{,}365)(93.61)]^2$$

$$= 62{,}058.0$$

$$S_T = y_1^2 + y_2^2 + \cdots + y_{18}^2 = 16.48^2 + 27.93^2 + \cdots + 93.61^2$$

$$= 73{,}397.8$$

$$S_e = S_T - S_\beta = 73{,}397.8 - 62{,}058.0$$

$$= 11{,}339.8$$

$$V_e = \frac{S_e}{k-1} = \frac{11{,}339.8}{18-1} = 667.0$$

$$\eta = 10 \log \frac{[1/(2.16)(10^9)]}{\dfrac{(62{,}058.0 - 11{,}339.8)}{667.0}}$$

$$= -73.70 \text{ dB}$$

The same methodology was used to calculate SN ratios for all 18 runs.

Response Analysis

The calculated SN ratio and beta values for each experimental run are displayed in Table 7. The average SN ratio for each control factor level is shown

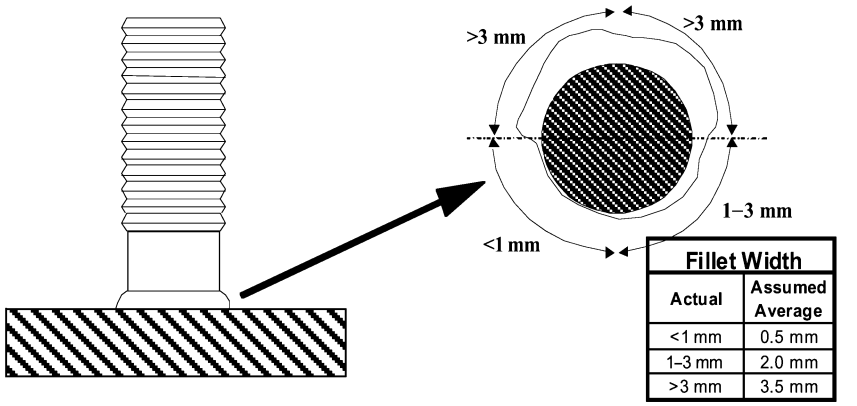

$$\text{Area} = (\text{Deg}_1/360)(16.48\ \text{mm}^2) + (\text{Deg}_2/360)(75.36\ \text{mm}^2) + (\text{Deg}_3/360)(148.36\ \text{mm}^2)$$

Where: Deg_1 = Total Degrees with Fillet <1 mm
Deg_2 = Total Degrees with Fillet 1–3 mm
Deg_3 = Total Degrees with Fillet >3 mm

Figure 3
Annular weld fillet area calculation

in Table 8. The data from the table are shown graphically in Figure 5. It can be seen that the spring damper (B), bushing material (C), and gas flow rate (H) have the largest effect on the SN ratio. It should also be noted that the dummy factor (G) had the lowest impact on the SN ratio, thus providing an indication that interactions between main effects are minimal.

Optimal Control Factor Settings

The optimal control factor settings were determined by selecting the combination of levels that maximize the SN ratio. Table 9 shows the optimum control factor levels and current process control factor levels predicted. The SN ratios predicted and gain expected are also presented in the table. Calculations for the values predicted are shown below.

optimal SN ratio predicted
$= B_2 + C_1 + H_2 - 2(\text{av. } \eta)$
$= (-67.76\ \text{dB}) + (-68.30\ \text{dB}) + (-68.36\ \text{dB}) - 2(-69.48\ \text{dB})$
$= -65.46\ \text{dB}$

current SN ratio
$= B_1 + C_2 + H_1 - 2(\text{av. } \eta)$
$= (-71.59\ \text{dB}) + (-69.38\ \text{dB}) + (-70.68\ \text{dB}) - 2(-69.48\ \text{dB})$
$= -72.69\ \text{dB}$

4. Beta Analysis

The value of β was calculated so that the squares of the distances between the right and left sides of the ideal function equation were minimized (least squares method). The calculation method is

$$\beta = \frac{1}{r}\left(\sum_{i=1}^{k} M_i y_i\right)$$

The β values calculated for each experimental run are displayed in Table 8. The average β values for each control factor level are shown in Table 10. The data from Table 10 are shown graphically in Figure 6. It can be seen that the spring damper (B) has the largest impact on β.

Table 5
Maximum torque prior to stud failure

	Maximum Torque (ft-lb)																	
	M_1		M_2		M_3		M_4		M_5		M_6		M_7		M_8		M_9	
Run	N_1	N_2	N_1	N_2	N_1	N_2	N_1	N_2	N_1	N_2	N_1	N_2	N_1	N_2	N_1	N_2	N_1	N_2
1	29.9	51.6	38.0	38.9	24.0	23.7	34.0	31.6	43.9	25.0	53.5	27.4	43.7	31.2	51.8	33.8	51.0	37.2
2	54.4	40.0	28.0	36.7	49.3	33.6	31.8	27.2	46.2	33.4	49.9	39.2	52.8	40.4	45.7	28.9	53.2	35.8
3	12.5	21.4	15.4	33.0	12.5	32.1	26.5	32.7	35.4	38.7	41.4	31.5	44.2	30.0	38.1	29.7	52.5	36.1
4	36.8	35.4	45.2	32.1	37.6	42.9	27.0	44.1	26.2	38.4	39.2	33.1	36.1	35.7	37.8	39.7	43.9	38.8
5	39.4	33.6	36.8	36.3	37.2	26.9	41.5	31.3	43.8	39.0	10.0	31.5	49.2	35.1	40.7	35.9	43.1	37.6
6	44.5	43.6	41.0	38.0	45.5	34.4	44.8	31.6	50.3	29.6	50.6	40.8	50.4	43.9	44.3	39.6	44.3	43.5
7	34.1	38.8	22.5	16.7	22.2	4.2	33.7	41.3	36.3	36.1	37.8	34.7	38.0	41.7	38.9	34.8	38.0	37.2
8	39.9	34.7	35.9	32.1	31.1	4.0	25.5	27.2	43.1	33.8	46.6	34.2	45.9	42.7	54.9	37.1	45.9	36.0
9	36.2	26.3	26.2	35.1	38.2	34.5	33.8	32.8	27.0	31.0	26.0	30.0	38.5	28.4	35.3	25.5	43.1	29.9
10	33.1	28.4	38.7	28.1	36.6	7.5	35.0	26.8	34.0	22.9	39.2	34.0	10.0	26.3	36.0	30.8	39.6	38.7
11	22.8	31.5	18.8	32.8	31.2	38.5	35.6	39.5	34.2	32.9	39.3	17.5	38.6	33.5	37.5	31.0	41.3	35.5
12	10.0	29.0	32.4	27.2	32.9	36.9	38.5	32.9	35.9	23.7	29.8	32.9	27.3	34.1	32.2	36.6	39.9	40.8
13	37.5	33.7	35.2	33.8	41.9	37.4	38.1	35.9	36.7	32.9	40.3	35.9	32.4	37.1	39.2	38.2	36.3	35.2
14	25.9	31.2	8.5	34.1	33.5	34.6	33.3	33.5	33.0	31.7	29.4	31.2	32.4	34.8	33.3	35.5	29.8	35.8
15	8.5	35.2	27.6	31.4	31.7	33.1	32.4	32.1	31.7	29.9	37.8	26.1	37.3	36.1	38.5	33.5	34.2	29.2
16	31.2	34.8	29.1	37.3	32.2	36.3	39.2	39.6	36.6	40.4	38.2	31.2	34.1	36.3	36.9	38.7	36.3	40.2
17	10.0	33.7	36.8	35.2	16.7	32.4	35.1	32.4	29.8	24.9	37.2	35.0	39.2	29.6	37.7	26.8	36.6	28.0
18	10.0	32.0	31.7	30.9	31.8	32.9	38.4	36.5	13.2	38.2	31.5	28.5	36.1	37.0	33.3	31.7	36.8	36.7

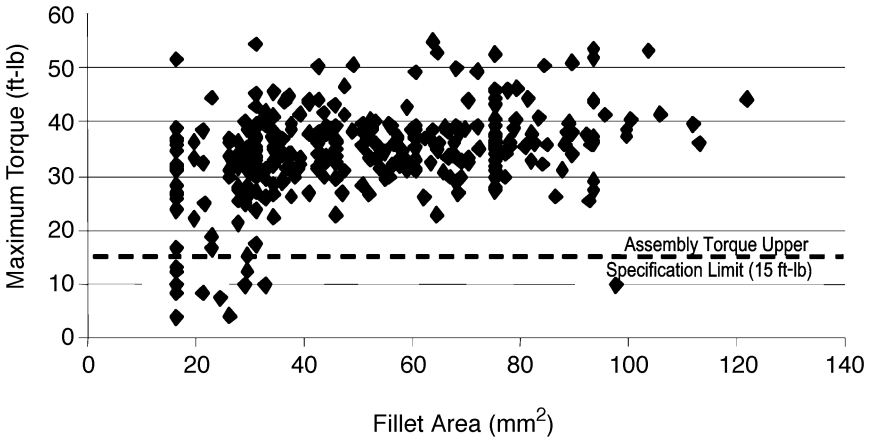

Figure 4
Weld fillet area versus maximum torque prior to stud failure

Table 6
Data for run 3

Trial	Actual Current (A)	Actual Time (s)	Voltage (V)	Energy, *M* (J)	Area, *y* Fillet (mm^2)
M_1	584.2	0.35	30.5	6,232	16.48
M_2	566.1	0.35	33.3	6,611	27.93
M_3	575.1	0.39	31.8	7,139	29.56
M_4	560.1	0.38	35.5	7,585	34.47
M_5	583.5	0.43	31.0	7,786	29.56
M_6	563.2	0.43	34.8	8,460	56.45
M_7	737.3	0.35	38.5	9,935	16.48
M_8	760.4	0.35	33.7	8,958	43.43
M_9	731.9	0.38	39.1	10,875	78.04
M_{10}	756.6	0.39	34.3	10,185	29.56
M_{11}	745.2	0.30	37.2	8,305	105.78
M_{12}	761.6	0.44	33.3	11,112	37.74
M_{13}	885.5	0.35	42.1	13,060	121.93
M_{14}	904.7	0.35	39.7	12,655	38.46
M_{15}	887.1	0.39	42.0	14,517	89.55
M_{16}	909.8	0.39	38.9	13,894	75.36
M_{17}	884.5	0.44	42.4	16,482	75.36
M_{18}	909.9	0.43	39.0	15,365	93.61

Table 7
SN ratio and beta values for each run

	Control Factor									
Run	***A***	***B***	***C***	***D***	***E***	***F***	***G***	***H***	**η**	**β**
1	1	1	1	1	1	1	1	1	−71.74	0.00542
2	1	1	2	2	2	2	2	2	−69.56	0.00544
3	1	1	3	3	3	3	3	3	−73.70	0.00536
4	1	2	1	1	2	2	3	3	−64.27	0.00476
5	1	2	2	2	3	3	1	1	−67.56	0.00478
6	1	2	3	3	1	1	2	2	−68.07	0.00438
7	1	3	1	2	1	3	2	3	−68.34	0.00397
8	1	3	2	3	2	1	3	1	−69.63	0.00382
9	1	3	3	1	3	2	1	2	−68.69	0.00420
10	2	1	1	3	3	2	2	1	−72.39	0.00522
11	2	1	2	1	1	3	3	2	−70.76	0.00504
12	2	1	3	2	2	1	1	3	−71.40	0.00540
13	2	2	1	2	3	1	3	2	−65.87	0.00450
14	2	2	2	3	1	2	1	3	−70.45	0.00417
15	2	2	3	1	2	3	2	1	−70.34	0.00426
16	2	3	1	3	2	3	1	2	−67.19	0.00421
17	2	3	2	1	3	1	2	3	−68.31	0.00407
18	2	3	3	2	1	2	3	1	−72.45	0.00347
							Average:		−69.48	0.00458

Table 8
SN ratio response table

	Control Factor							
Level	***A***	***B***	***C***	***D***	***E***	***F***	***G****	***H***
1	−69.06	−71.59	−68.30	−69.02	−70.30	−69.17	−69.51	−70.69
2	−69.91	−67.76	−69.38	−69.20	−68.73	−69.64	−69.50	−68.36
3	—	−69.10	−70.78	−70.24	−69.42	−69.65	−69.45	−69.41
Δ	0.84	3.83	2.48	1.22	1.57	0.48	0.06	2.33

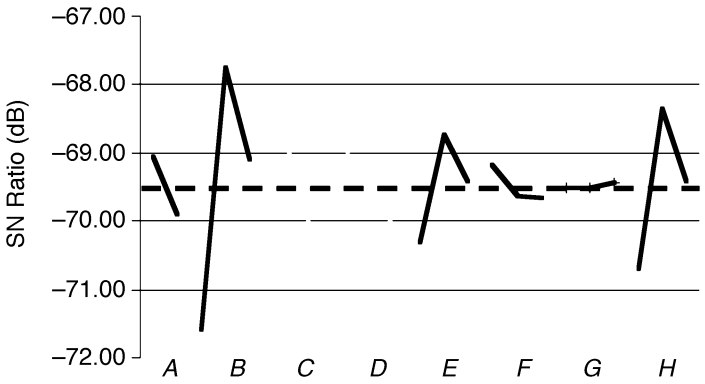

Figure 5
SN ratio effect plot

Table 9
Optimal control factor settings and SN ratio predictions

Configuration	Gas Mixture	Spring Damper	Bushing Material	Preflow Gas Duration (s)	Postflow Gas Duration (s)	Plunge Depth (in.)	Gas Flow Rate (ft^3/h)	SN Ratio Predicted (dB)
Optimal	90/10	Weak	Plastic	0.50	0.50	0.040	20	−65.46
Current	98/2	None	Steel	0.50	0.50	0.070	10	−72.69
							Gain predicted:	7.23

Table 10
Beta response

	Control Factor							
Level	*A*	*B*	*C*	*D*	*E*	*F*	*G**	*H*
1	0.00468	0.00531	0.00468	0.00463	0.00441	0.00460	0.00470	0.00450
2	0.00448	0.00448	0.00455	0.00459	0.00465	0.00454	0.00456	0.00463
3	—	0.00396	0.00451	0.00453	0.00469	0.00460	0.00449	0.00462
Δ	0.00020	0.00136	0.00017	0.00010	0.00028	0.00006	0.00020	0.00013

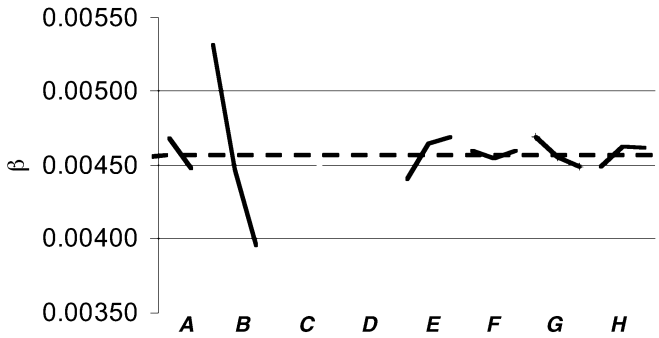

Figure 6
Beta effect plot

Table 11
Predicted versus confirmed results

	Predicted		Confirmed	
	SN Ratio (dB)	β	SN Ratio (dB)	β
Optimal	−65.46	0.00458	−66.85	0.00420
Current	−72.69	0.00520	−73.23	0.00518
Gain	7.23		6.38	

Beta Predictions

In the production environment, the input energy will be set to an optimum level and held constant. Therefore, β is relatively unimportant in this experiment. However, a comparison of predicted β values to confirmed values will provide increased insight into the validity of the experimental results. Therefore, β values were predicted using the optimal control factor levels as identified in the SN ratio analysis. Beta predictions are as follows:

Optimal: 0.00458

Current: 0.00520

Calculations for the values predicted are:

optimal SN ratio predicted
$= B_2 + C_1 + H_2 - 2(\text{av. } \eta)$
$= 0.00448 + 0.00463 + 0.00463 - (2)(0.00458)$
$= 0.00458$

current SN ratio
$= B_1 + C_2 + H_1 - 2(\text{av. } \eta)$
$= 0.00531 + 0.00455 + 0.00450 - (2)(0.00458)$
$= 0.00520$

5. Confirmation Test

The confirmation test was conducted in three steps:

1. Testing at *current* control factor settings across all 18 energy input levels:

   Control factor settings: $A_1B_1C_2D_1E_1F_2H_1$

2. Testing at *optimal* control factor settings predicted across all 18 energy input levels:

   Control factor settings: $A_1B_2C_1D_2E_2F_1H_2$

3. Testing at *optimal* control factor settings predicted at the *optimum* energy input level:

Table 12
Constant-set-point versus full-energy input range

Confirmed Optimal	SN Ratio (dB)	β
Full energy input range	−66.85	0.00420
Constant set point	−66.86	0.00475

Control factor settings: $A_1B_2C_1D_2E_2F_1H_2$

Signal factor settings: 840 A, 0.35 s

Each confirmation test was conducted in exactly the same manner as each run in the original L_{18} experimental array. SN ratio results from the initial two steps of the confirmation run are compared to their predicted values in Table 11. The confirmed results compare favorably to the values predicted.

The 6.38-dB gain between current and optimal conditions translates into a 52.1% reduction in energy transformation variability, as shown by the following calculation:

$$\text{variability reduction} = 1 - 0.5^{\text{gain}/6} = 1 - 0.5^{6.38/6} = 52.1\%$$

Based on weld fillet area, torque testing, and general visual inspection results of studs welded under optimal parameter settings, the team chose 840 A and 0.35 s as the most desirable signal factor settings. Therefore, a third confirmation run was performed at a constant 840 A, 0.35 s set point. Even though the input energy set point was held constant, the actual energy input varied from stud to stud due to the inherent variability of the power supply. The one positive effect of this inherent variability was that it enabled calculation of a SN ratio and β for the run. Table 12 shows a comparison of the results of the constant-set-point run and the original optimal condition confirmation run utilizing the full input energy range. It can be observed that the results of the runs were virtually identical.

Figure 7 shows the torque testing results from studs welded under optimal control factor settings and the constant input energy setpoint of 840 A, 0.35 s. For all studs in this run, the weld yield strength was greater than the stud material yield strength.

The average observed maximum torque prior to failure (39.6 ft-lb) is 2.6 times larger than the assembly torque upper specification limit. The optimal process data exhibit a state of statistical control; therefore the process capability index (C_p) can be calculated as follows:

$$C_p = \frac{\text{average max. torque} - \text{assembly torque upper spec. limit}}{\sigma}$$

where σ is the estimated standard deviation (mRbar/D_2 method). Therefore, for the optimal process,

$$C_p = \frac{39.6 - 15.0}{(3)(2.72)} = 9.03$$

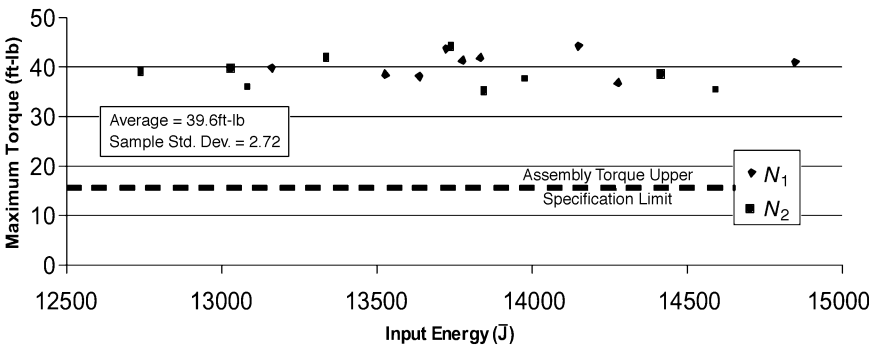

Figure 7
Maximum torque prior to stud failure: Optimal process

6. Conclusions

Process parameter optimization utilizing robust design methodology clearly resulted in a substantial improvement in the gas-arc welding process. The optimal combination of control factor settings was determined, resulting in a 52.1% process variability reduction and an average stud weld strength of 2.6 times the level required by the assembly operation. Of the seven control factors tested, only two factors had been set at their optimal level. Additionally, the preexperiment welding energy input settings (700 A, 0.4 s) were found to be suboptimal. Implementation of the optimized process parameters is expected to result in significant cost savings (greater than $30,000), due to the elimination of a secondary welding operation and a significant reduction in downstream stud strength failures.

References

American Supplier Institute, 1998. *Robust Design Using Taguchi Methods: Workshop Manual*. Livonia, MI: American Supplier Institute, pp. I1–II36.

American Welding Society, 1993. *ANSI/AWS C5.4-93: Recommended Practices for Stud Welding*. Miami, FL: American Welding Society.

Yuin Wu, 1999. *Robust Design Using Taguchi Methods*. Livonia, MI: American Supplier Institute, pp. 47–51.

This case study is contributed by Jeff Stankiewicz.